Bioorthogonal chemical engineering of rAAV capsid: Advancing gene therapy targeting using proteins

Maia Marchand,[1,2,*] Sébastien Depienne,[2] Mohammed Bouzelha,[1] Karine Pavageau,[1] Roxane Peumery,[2] Denis Loquet,[2] Dimitri Alvarez-Dorta,[2,3] Mickaël Guilbaud,[1] Mikaël Croyal,[4,5] Aurélien Dupont,[6] Oumeya Adjali,[1] Sébastien G. Gouin,[2] David Deniaud[2,*] & Mathieu Mével[1,2,*].

[1]Nantes Université, TaRGeT, Translational Research for Gene Therapies, CHU Nantes, INSERM, UMR 1089, F-44000 Nantes, France.
[2]Nantes Université, CNRS, CEISAM, UMR 6230, F-44000 Nantes, France.
[3]Capacités SAS, Nantes, France.
[4]Nantes Université, CNRS, INSERM, Institut du thorax, F-44000 Nantes, France.
[5]Nantes Université, CHU Nantes, Inserm, CNRS, SFR Santé, Inserm UMS 016, CNRS UMS 3556, F-44000 Nantes, France.
[6]CNRS, INSERM, BIOSIT_UAR 3480, Univ Rennes, Inserm 018, F-35000 Rennes, France.

*Corresponding authors:

maia.marchand@univ-nantes.fr
david.deniaud@univ-nantes.fr
mathieu.mevel@univ-nantes.fr

ABSTRACT

We report the chemical conjugation of recombinant Adeno Associated Virus (rAAV) capsid with various functionalities, including proteins, using a bioorthogonal strategy. rAAVs were azido-coated or DBCO-coated by chemically modifying lysine or tyrosine residues. Lysine residues were modified using a phenyl isothiocyanate anchor, and tyrosine residues using either an aryldiazonium salt or a *N*-methyl luminol derivative. We demonstrate anchor-dependent labelling levels, as observed with biochemical assays and mass spectrometry. Strain-promoted azide-alkyne cycloaddition (SPAAC) was then implemented and evaluated on the rAAV to append functionalities such as fluorescein, biotin and carbohydrates to the azido-coated capsids. We confirmed the efficiency of the bioorthogonal reaction and observed a stronger reactivity with dibenzylcyclooctyne (DBCO) compared to bicyclononyne (BCN). The optimized SPAAC reaction was finally used to label the viral vectors with two relevant nanobodies targeting specific immune cell receptors (CD62L and CD45). *In vitro* transduction assays conducted with one rAAV-nanobody conjugate demonstrated the promising targeting properties of these chemically modified vectors. Thus, we anticipate that this strategy will positively impact the field of rAAV capsid engineering and contribute in tissue-specific targeting for the optimisation of gene therapy treatments.

KEYWORDS

rAAV, SPAAC, bioorthogonal click chemistry, bioconjugation, nanobody, gene therapy.

INTRODUCTION

In recent years, recombinant Adeno Associated Viruses (rAAVs) have emerged as one of the most promising vector candidates in clinical studies for *in vivo* gene therapy[1,2]. This is primarily attributed to their ability to transduce a diverse array of cells and tissues with persistent transgene expression, as well as a good safety profile[3]. Patients suffering from metabolic to retinal disorders are now treated with rAAVs using a single injection protocol[4–6].

Thirteen AAV serotypes were originally described in the literature[3,7]. For each one, preferentially transduced tissues were identified[8], such as rAAV9 which demonstrated interesting gene delivery capabilities in the brain[9]. However, these tropisms remain overly broad, lacking tissue specificity, which results in off-target expression and reduced efficiency. To address this issue, high doses of vectors need to be administrated to the patient, enhancing the risk of immune toxicity[10], challenging the large scale production of vectors[11] and leading to expensive treatments.

As a key approach to redirect tropism and improve the therapeutic index, the design of the viral capsid is extensively explored. Among the strategies, chimeric vectors have been produced by mixing viral proteins from different serotypes to take advantage of their distinct characteristics[12,13]. Additionally, larger rAAV libraries were generated through directed evolution approaches, shuffling methods or peptide display techniques[14,15]. A prominent example has been the rAAV-PHP.eB capsid, which demonstrated an enhanced transduction in the central nervous system[16]. Nevertheless, without rational design, such strategies rely on screening experiments in *in vivo* models, which may not always accurately represent the actual rAAV biodistribution in human[17]. More rational approaches have also been explored including specific genetic insertion[18–20]. Non-natural amino acids bearing specific anchors were incorporated into VP viral protein (VP) sequences to further append relevant small molecules or oligonucleotides using bioorthogonal reactions[21–25]. Additionally, the highly specific targeting properties of proteins and peptides have also been exploited. For instance, a noteworthy construction involving DARPins fused to the VP2 *N*-terminus has been described as a relevant strategy to redirect the rAAV toward HER2/neu$^+$ cells[26]. Genetic engineering continues to provide precise control over the site and degree of modification, which is of significant importance for the rAAV properties. However, the production process needs adaptation for each case, and the vectors often suffer from low titers[27].

Alternatively, recent investigations, including our previous works, have explored the direct chemical modification of rAAV vectors. Residues such as lysine (K) or tyrosine (Y) composing the proteins of the AAV capsid, have been bioconjugated with targeting or imaging small molecules (*e.g.* carbohydrates, radionuclides, fluorophores) resulting in a promising improvement or monitoring of the transduction of selected tissues[28–30]. However, the conjugation of complex structures, particularly proteins, inherently cannot be explored using this direct bioconjugation strategy.

In this study, we demonstrated and optimized a direct chemical sequence featuring biorthogonality to access rAAV-protein conjugates as a faster and easier alternative to genetic manipulations. We first achieved the obtention of an azido-coated rAAV using chemoselective bioconjugation on K or Y residues, to evaluate and compare potential efficiency differences. Phenyl isothiocyanate and aryl diazonium salt were the bioconjugation anchors selected for K and Y modification, respectively, owing to their non-disruptive and efficient modification of rAAVs[28,30]. Additionally, we explored the functionalization of rAAVs with a *N*-methyl luminol (NML) derivative using the Y-targeting click-electrochemistry strategy recently reported by our group for viral and cell surfaces labelling[31]. Azido-coated rAAVs were successfully obtained in all cases, with labelling levels dependent on the bioconjugation strategy. Subsequently, post-functionalization using the bioorthogonal strain-promoted azide-alkyne cycloaddition (SPAAC)[32] was illustrated and optimized with cyclooctyne-derivatized small molecules (fluorescein, biotin, *N*-acetylgalactosamine). Interestingly, DBCO (dibenzylcyclooctyne) exhibited a significantly higher reactivity than BCN (bicyclononyne) in our model. On the other hand, the chemical bioconjugation of rAAV with the valuable DBCO click handle was successfully conducted, which, to the best of our knowledge, has never been reported before. Subsequently, SPAAC post-functionalization using a synthetic azido-derivatized fluorescent probe was similarly proven at the capsid scale, highlighting the possibility to easily and rapidly label rAAVs with a broad range of azido-tagged functionalities. With the optimized bioorthogonal sequence in hands, two biologically relevant nanobodies anti-CD45 and anti-CD62L (targeting specific immune cells markers[33,34]) were successfully covalently linked to the viral capsid to afford rAAV-nanobodies conjugates with conserved transduction capacity in HeLaT cells. More interestingly, the transduction in the presence of the cell-binding inhibitor heparin was partially maintained in the CD45-expressing cell line Jurkat when rAAV was labelled with the anti-CD45 moiety, highlighting the therapeutic prospect of the bioorthogonal strategy. These promising results contribute to the advancement of next-generation capsid engineering, paving the way for tissue-targeted gene therapy.

RESULTS AND DISCUSSIONS

Obtention of azido-rAAV2

Our investigations started with the chemical labelling of the rAAV capsid with azido moieties. Considering the potential impact of amino acid selection and bioconjugation anchors on both the efficiency and level of functionalization (affecting the resulting vector profiles[28,30]), we compared several strategies. Three distinct anchors were designed, based on previous reports where rAAV labelling with carbohydrates has been successfully achieved on K and Y residues[31,35]. The azido moiety was associated with a phenyl isothiocyanate for K modification, an aryl diazonium salt for the Y one and a *N*-methyl luminol to explore electrochemical Y-conjugation. Their synthesis is outlined in Scheme 1. We first carried out a three-step synthetic route to obtain the azido-amino linker **4** using triethylene glycol. After tosylation of the two alcohol groups of compound **1**, and substitution with sodium azide, we performed the Staudinger reduction of only one of the azido moieties thanks to biphasic conditions. To obtain the K targeting anchor **Lys-N_3**, a one-step *N*-functionalization of the amine **4** with bitoscanate was carried out. To synthesize the azido-aniline derivative **6**, the same intermediate **4** was used to perform a peptide coupling with 4-aminobenzoic acid protected with a BOC group, which was removed in an additional deprotection step with TFA. This molecule **6** served as the

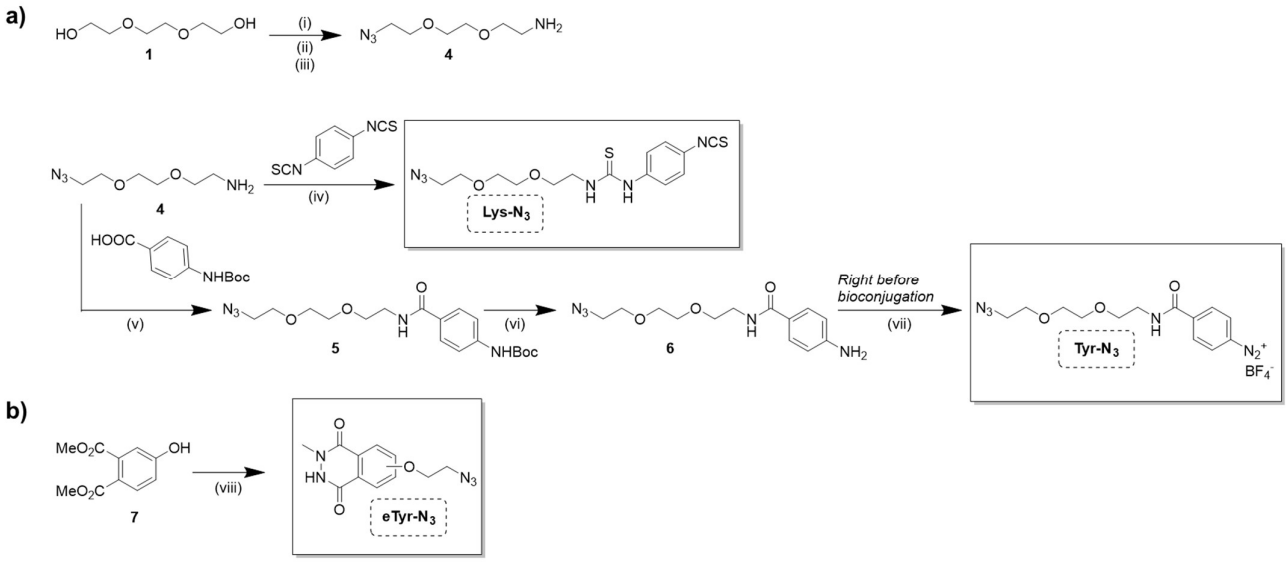

substrate for diazonium-activation (**Tyr-N_3**) just before the bioconjugation reaction. Additionally, we carried out a previously reported four-step synthesis[31] to obtain from **7** the azido-NML derivative **eTyr-N_3**, the anchor being electro-oxidized to label tyrosine.

Scheme 1: Synthesis of the bioconjugation anchors. (a) **Lys-N_3** for K functionalization, **Tyr-N_3** for chemical Y functionalization, (b) **eTyr-N_3** for Y electrochemical functionalization. (i) TsCl, Et_3N, DCM, RT, 18 h (69 %); (ii) According Budin *et al.* (2010)[36]: NaN_3, DMF, 70°C, 18 h (quant.); (iii) According to Goswami *et al.* (2013)[37]: PPh_3, Et_2O, 5 % HCl, RT, 20 h (84 %); (iv) DMF, RT, 4 h (88 %); (v) HBTU, DMAP, DMF, RT, 3 h 30 (80 %); (vi) TFA, DCM then basic resin, RT, 4 h (96 %); (vii) HBF_4, tBuONO, dPBS, RT, 5 min (quant.); (viii) 4-step synthesis by Depienne *et al.* (2021)[38].

For the bioconjugation step, we selected rAAV2 vectors, a highly studied and characterized serotype[7]. Conditions using 1^E5 equivalents of **Tyr-N_3** and **Lys-N_3** (Fig. 1.a) and a concentration of 0.5 mM of **eTyr-N_3** were chosen according to the reported reactivity of the corresponding anchors (Fig. 1.b). The bioconjugation reactions were performed as follows: **Lys-N_3** was directly co-incubated with rAAV2, **Tyr-N_3** was obtained from **6** by the action of hexafluoroborate (HBF_4) followed by *tert*-butyl nitrite (*t*BuONO), and **eTyr-N_3** was electro-oxidized at 750 mV *vs* Ag/AgCl. The resulting vectors were characterized using various analytical techniques. The A20 antibody was employed in the dot blot assay to discern any alterations in the capsid 3D structure, confirming that the conjugation step did not induce structural modifications (Fig. 1.c). To validate the azido labelling of rAAVs, we substituted the antibody in the dot blot analysis with fluorescein conjugated to the BCN structure (**BCN-F**). For any azido moieties present on viral proteins, a SPAAC reaction would occur directly on the nitrocellulose membrane, resulting in a fluorescent signal (Fig. 1.c). Satisfyingly, we confirmed the functionalization of the three azido-conjugated rAAV2. A strategy-dependent level of labelling was observed with a notably stronger fluorescence signal with lysine (**AAV2-Lys-N_3**) and electro-tyrosine modification (**AAV2-eTyr-N_3**) as compared to chemical tyrosine modification (**AAV2-Tyr-N_3**). The effective bioconjugation of **AAV2-Lys-N_3** and **AAV2-eTyr-N_3** was further supported by mass spectrometry analyses. Azido-labelled rAAV2 were injected into an UPLC column without any denaturation treatment. We focused on the mass spectrum corresponding to VP3, the smallest and most abundant of the three viral proteins (VP1-3) composing the capsid[39]. For **AAV2-Lys-N_3**, the deconvoluted mass spectrometry profile of VP3 confirmed the presence of the protein with zero, one, or two covalently conjugated anchors (Fig. 1.e). Electro-conjugation exhibited a higher degree of functionalization, as the native VP3 protein was not detectable, with an average of four modifications displayed (Fig. 1.f). Unfortunately, we could not confirm the labelling of **AAV2-Tyr-N_3** by mass spectrometry, likely due to a lesser number of modified proteins.

To confirm that the labelled vectors conserved their functional integrity, we evaluated their infectivity on HeLa cells. Cells were co-incubated with azido-functionalized rAAV2 carrying an Enhanced Green Fluorescent Protein (eGFP) reporter gene expression cassette under the control of a ubiquitous promoter at a multiplicity of infection (MOI) of 1^E3, and the percentage of fluorescent cells was measured after 48 hours by flow cytometry (Fig. 1.d). No significant loss of transduction was observed, indicating that neither the bioconjugation conditions nor the azido coating affected GFP expression.

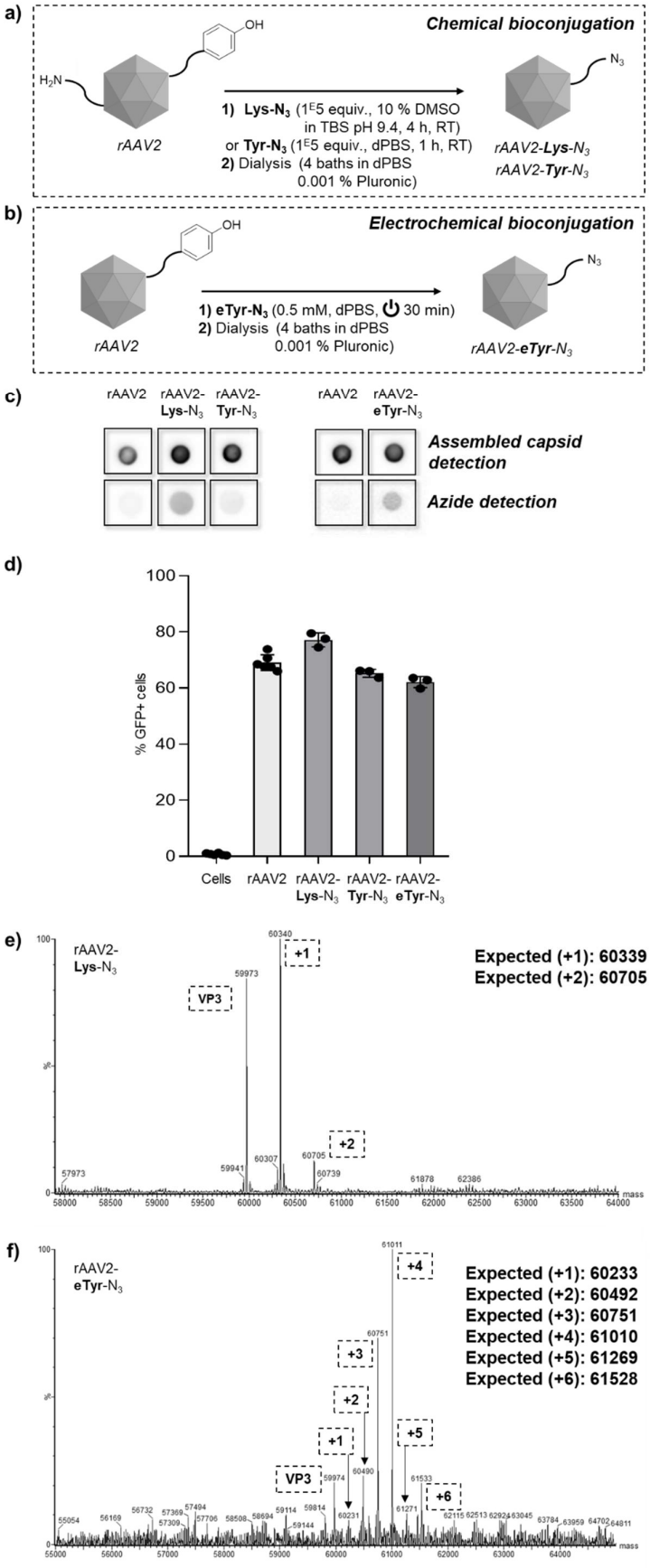

Figure 1: Bioconjugation of rAAV2 with azido derivatives and characterization of the obtained vectors. a) rAAV2 bioconjugation with **Lys-N_3** or **Tyr-N_3** using 1^E5 equiv. in aqueous buffers. b) rAAV2 electro-bioconjugation after an *in situ* electro-oxidation (750 mV *vs* Ag/AgCl) of **eTyr-N_3** for 30 min at 0.5 mM in dPBS. c) Dot Blot analysis of viral vectors to detect (up lane, 2^E10 vg) the assembled capsid using the A20 antibody followed by secondary revelation using an anti-mouse-HRP antibody or to detect (down lane, 3^E10 vg) the azido moieties using **BCN-F**. (d) Evaluation of the transduction efficiency in HeLaT of modified rAAV2 carrying eGFP reporter gene expression cassette under the control of a ubiquitous promoter. GFP-positive HeLaT quantification by flow cytometry 48 h after infection at a MOI of 1^E3 (data are shown as mean ± SD of three distinct samples (n=3)). e) and f) Analysis by mass spectrometry of r**AAV2-Lys-N_3** and r**AAV2-eTyr-N_3**. Vectors were analyzed without any denaturation step. Mass profiles were obtained after migration on an UPLC column and deconvolution of the VP3 corresponding peak (MW (**Lys-N_3**) = 366.46 g/mol and MW (**eTyr-N_3**) = 261.24 g/mol).

Comparison of the reactivity of two cyclooctynes

Various cyclooctynes have been reported in the literature for their efficient reaction with azido moieties in a bioorthogonal manner[40]. In this study, we focused on BCN and DBCO to explore the post-functionalization of azido-labelled rAAV2 using the SPAAC reaction. Their reactivity was assessed on **rAAV2-Lys-N_3** over a period of one hour using 10 µM of a fluorescent cyclooctyne in each case (Fig. 2.a). Dot blot analysis, based on direct fluorescence measurement, showed a stronger signal with the DBCO structure compared to BCN while no modification of the 3D structure was observed with A20 detection (Fig. 2.b). The difference in post-functionalization was further supported by SDS-PAGE analysis. The three specific viral proteins constituting the capsid (VP1, VP2, and VP3) were unambiguously modified with **DBCO-F**, as three distinct fluorescent bands corresponding to the molecular weights of these proteins were observed. These bands were clearly not detected with the **BCN** scaffold (Fig. 2.c). It is noteworthy that two VP3 populations were greatly separated on the silver staining of DBCO modified vectors (red arrow on Fig. 2.d). We can hypothesize that the larger one may correspond to a modification of the VP3 unit, providing additional evidence of the successful SPAAC reaction. Given the observed difference in reactivity, DBCO derivatives were chosen for the post-functionalization of azido-labelled rAAV2, and the fluorescein-coating of **rAAV2-Tyr-N_3** and **rAAV2-eTyr-N_3** was explored in Fig. S13.

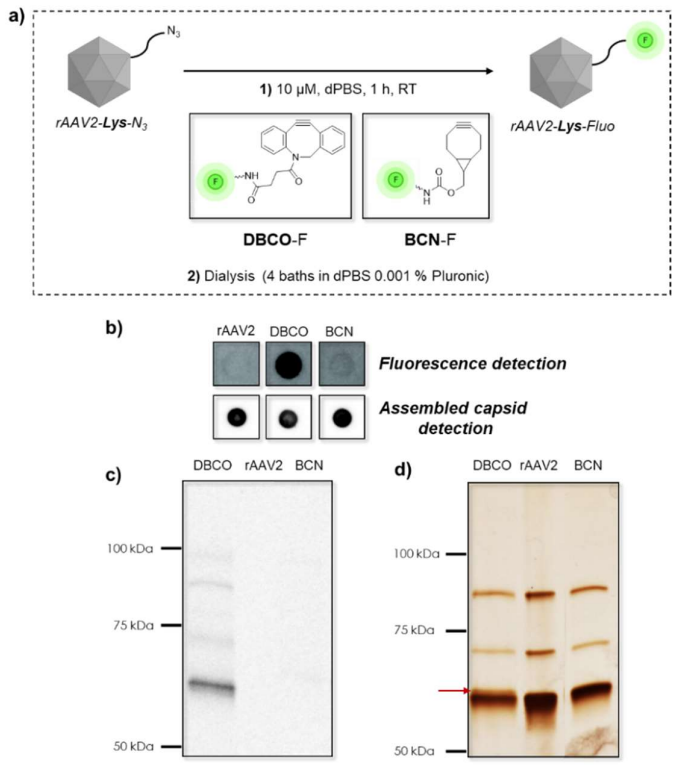

Figure 2: Comparison of the efficiency of BCN and DBCO cyclooctynes to post-functionalize azido-vectors. a) SPAAC reaction for **rAAV2-Lys-N_3** post-functionalization using **BCN-F** and **DBCO-F** at 10 µM for 1 h. b) Dot Blot analysis of viral vectors to detect (up lane, 1.5^E10 vg) the covalent linkage of fluorescein by direct fluorescence measurement or to detect (down lane, 2^E10 vg) the assembled capsid using the A20 antibody followed by secondary revelation using an anti-mouse-HRP antibody. c) Detection of fluorescein on capsid proteins with direct fluorescence measurement after denaturation and migration by SDS-PAGE of modified or non-modified rAAV2 (1.5^E10 vg). d) Silver staining of capsid viral proteins after denaturation and SDS-PAGE migration of modified or non-modified rAAV2 (1.5^E10 vg).

Azido-rAAV2 post-functionalization with DBCO-derivatized small molecules

To further demonstrate the rapid and efficient access to a variety of functionalized rAAV2, we expanded the SPAAC reaction to include biotin and GalNAc derivatives, using **DBCO-B** and **DBCO-G** respectively (structures and syntheses are provided in the Supplementary Information, Fig. 3.a). Biotin is widely recognized in the literature as an effective molecular label[41], while GalNAc serves as hepatocyte targeting moiety[42].

Each modification was specifically studied using dot blot assays. Streptavidin was employed to detect biotin and the soybean lectin specific to the GalNAc carbohydrate was used. We successfully confirmed the SPAAC reaction with the two functionalities on the three azido-coated rAAV2 (Fig. 3.b). The results corroborated our previous findings. Notably, a higher degree of post-modification was obtained from the more azido-labelled **AAV2-Lys-N_3** and **AAV2-eTyr-N_3**, compared to **AAV2-Tyr-N_3**. Despite a very low concentration of rAAV2 (C_{AAV} is approximately 1 nM), a higher number of azido groups on the capsid resulted in a higher degree of post-functionalization. This observation highlights the interesting opportunity for grafting modulation. Importantly, unmodified rAAV2 were reacted under the same conditions with the derivatized DBCO which showed a total absence of signals detection (Fig.

S15.a). rAAV2 vectors were also analyzed with a A20 dot blot assay, and no modifications in capsid integrities were noticed (Fig. 3.b, lane 2). Functionalized viral proteins were additionally visualized by SDS-PAGE followed by silver staining (Fig. 3.c). Consistent with previous observations, this assay demonstrated that the electrochemically-labelled AAV was the most highly post-functionalized vector in all cases. For **rAAV2-eTyr-B**, the modification may even be too drastic as it is difficult to clearly identified which band corresponds to which protein. On the contrary, despite a similar working concentration (50 µM for **DBCO-B** and **DBCO-G**), we can clearly identify the viral proteins on **rAAV2-eTyr-G** SDS-PAGE profile**,** which can indicate a difference in reactivity between the DBCO constructs. Furthermore, the profile particularly echoes the mass spectrometry analysis presented in Figure 1.f. Indeed, three distinct levels of VP3 modification could be observed (red arrows in Fig. 3.c), providing an evidence that poly-modifications of the proteins is possible.

Gratifyingly, in HeLa cells, almost all functionalized vectors induced GFP production at levels comparable to unmodified rAAV2 (Fig. S14.c). Unsurprisingly, the exception was **rAAV2-eTyr-B**, which showed lower transduction efficacy. Considering its SDS-PAGE profiles, the observed differences in transduction could be attributed to a too high degree of functionalization of the capsid with crowded and/or hydrophobic structures. Both the duration of SPAAC reaction and the concentration of DBCO derivatives seem to be key factors that can be adjusted to fine-tune capsid engineering. Nevertheless, all the data mentioned underscore the interest of the three obtained azido-labelled AAVs for accessing a variety of post-functionalized vectors.

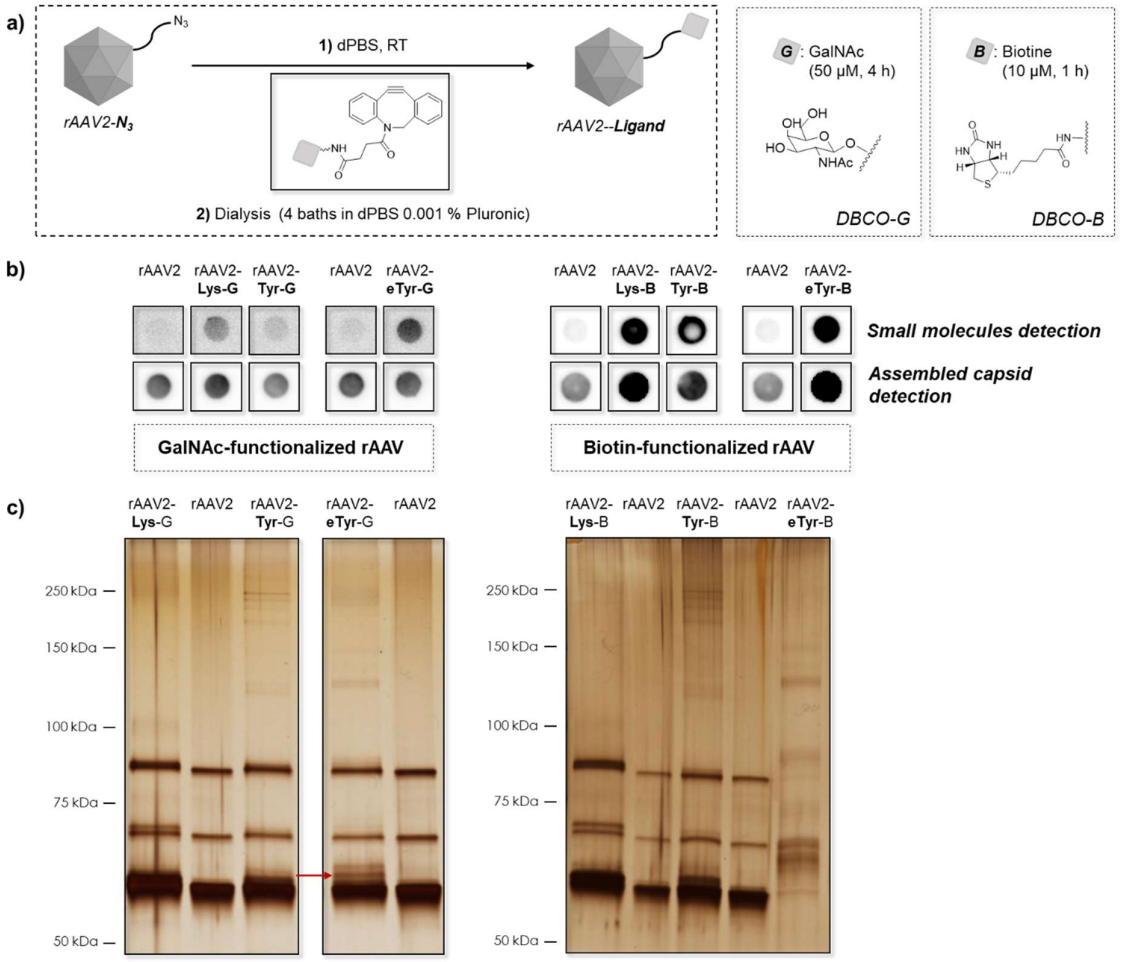

Figure 3: SPAAC reaction on azido-rAAV2 with DBCO-derivatized small molecules. a) SPAAC reaction for **rAAV2-Lys-N$_3$**, **rAAV2-Tyr-N$_3$** and **rAAV2-eTyr-N$_3$** using a DBCO-derivatized *N*-acetylgalactosamine (**DBCO-G**) and a DBCO-derivatized biotin (**DBCO-B**). b) Dot Blot analysis of viral vectors to detect (up line) the covalent labelling of the capsids with DBCO derivatives or to detect (down lane, 1^E10 vg) the assembled capsid using the A20 antibody followed by secondary revelation using an anti-mouse-HRP antibody. GalNAc labelling was detected (2^E10 vg) using a FITC-conjugated Soybean Agglutinin (SBA) lectin followed by secondary revelation using an anti-FITC-HRP antibody. Biotin labelling was detected (1^E10 vg) with an HRP-conjugated Streptavidin. c) Silver staining of capsid viral proteins after denaturation and SDS-PAGE migration of modified or non-modified rAAV2 (1.5^E10 vg).

DBCO vector and post-functionalization with an azido derivative

DBCO-labelled vectors can also be developed as interesting targets to expand the scope of post-functionalization. Indeed, azido derivatives can sometimes be more accessible than their corresponding DBCO counterparts. For instance, non-natural azido amino acids can be easily incorporated into protein sequences with control over the number and sites of incorporation, thanks to significant advancements in the field of genetic engineering[43]. DBCO derivatives can sometimes be difficult to synthesize, and stability and solubility issues may arise. In such cases, replacing them with an azido group in the synthetic route would represent an interesting alternative solution. To maximize the potential of chemical conjugation for rAAV engineering, we explored reversing the roles of the two click partners and investigated the possibility of obtaining DBCO-conjugated rAAVs.

Due to solubility issues of DBCO associated with the lysine conjugating moiety, we only investigated the labelling with the tyrosine chemical anchor. The desired aniline **12** was synthesized in a single step of peptide coupling (Fig. 4.a). The corresponding diazonium salt **Tyr-DBCO** was obtained in DMSO just before the conjugation step, and $1^{E}5$ equivalents were added to the rAAV2 mixture (Fig. 4.b). Similar to azido-rAAVs, we carried out a dot blot analysis using an azido-fluorescein derivative (**N_3-F**) to perform the SPAAC reaction on the nitrocellulose membrane, confirming the presence of the DBCO moiety. As shown in Fig. 4.c, the fluorescent signal clearly demonstrated the covalent coupling of the capsid with the DBCO moiety, without affecting the 3D structure, as indicated by the additional A20 staining. The DBCO vector was characterized by mass spectrometry, and the obtained profile confirmed the bioconjugation of rAAV2. Specifically, we observed that VP3 was partially mono-bioconjugated (Fig. 4.d).

To validate the post-functionalization of DBCO vectors, we explored the conjugation of **N_3-F** (100 µM). Interestingly, on the silver staining analysis shown in Fig. 4.e, three additional bands were clearly observed above the three viral proteins (red arrows). Combined with the intense fluorescent signal observed in SDS-PAGE analysis with fluorescence revelation in Fig. 4.f, this unequivocally demonstrates the successful and efficient probe labelling. DBCO-coated rAAVs complement the previously described azido vectors, contributing to the development of a broad-spectrum functionalization strategy for rAAV capsid engineering.

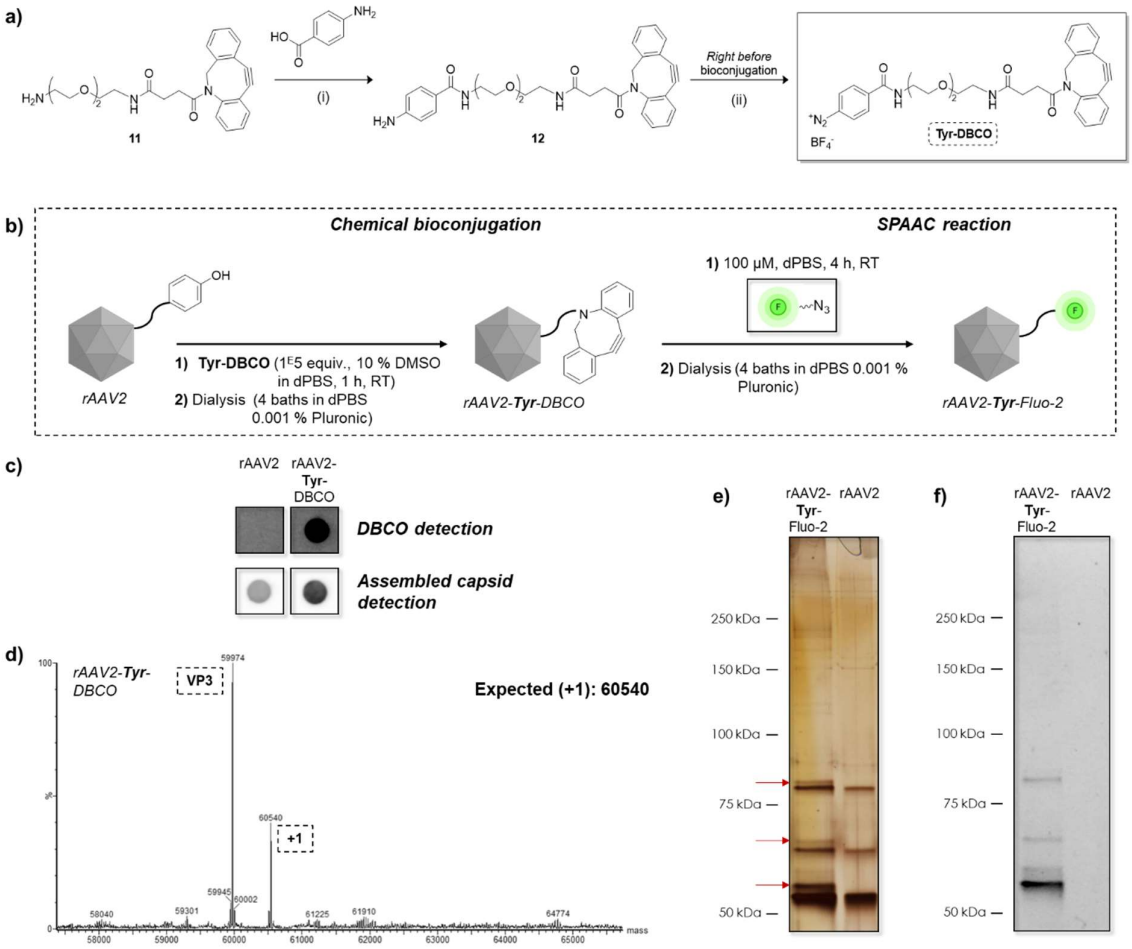

Figure 4: Obtention of DBCO-labelled rAAV2: synthesis of the tyrosine anchor, characterization of the obtained vector and post-functionalization with N_3-F. a) Synthesis of the **Tyr-DBCO** compound. (i) HBTU, DMAP, DMF, RT, 4 h (51%); (ii) HBF_4, tBuONO, DMSO, RT, 5 min (quant.). b) rAAV2 bioconjugation with **Tyr-DBCO** using 1^E5 equiv. in dPBS and SPAAC reaction using an azido-derivatized fluorescein (**N_3-F**) at 100 µM. c) Dot Blot analysis of viral vectors to detect (up lane, 3^E10 vg) the DBCO moieties using **N_3-F** or to detect (down lane, 1^E10 vg) the assembled capsid using the A20 antibody followed by secondary revelation using an anti-mouse-HRP antibody. d) Analysis by mass spectrometry of **rAAV2-Tyr-DBCO**. Vectors were analyzed without any denaturation step. Mass profiles were obtained after migration on an UPLC column and deconvolution of the VP3 corresponding peak (MW (**Tyr-DBCO**) = 566.64 g/mol). e) Silver staining of capsid viral proteins after denaturation and SDS-PAGE migration of **N_3-F** modified and non-modified rAAV2 (1.5^E10 vg) f) Detection of fluorescein on capsid proteins with direct fluorescence measurement after denaturation and SDS-PAGE migration of fluorescein modified and non-modified rAAV (1.5^E10 vg).

rAAV2 post-functionalization with proteins

The effective post functionalization of azido-rAAV2 or DBCO-rAAV2 was initially validated with small molecules. However, larger structures, including biomolecules, can also possess interesting properties, particularly in terms of targeting[44,45]. For instance, nanobodies have been extensively explored due to their size, ease of production, and high specificity, making them powerful tools for tissue-specific addressing[46]. In this study, we explored the possibility of post-functionalizing the azido vectors **rAAV2-Lys-N_3** and **rAAV2-eTyr-N_3** with two biologically relevant nanobodies: anti-human CD62L and anti-human CD45. The former interacts with the cell adhesion molecule CD62L which is implicated in immune cell

interactions[47], while the latter binds to the well-described leukocyte marker CD45[48]. The SPAAC reaction was performed with DBCO-derivatized nanobodies (Fig. 5.a) considering the demonstrated higher reactivity of azido-rAAV2 with DBCO compared to BCN (Fig. 2). Silver staining analysis of **rAAV2-Lys-CD62L**, **rAAV2-eTyr-CD62L**, **rAAV2-Lys-CD45**, and **rAAV2-eTyr-CD45** unambiguously revealed a new protein band slightly above 75 kDa (indicated by red arrows in Fig. 5.b). This supports the successful functionalization of the corresponding nanobodies (16 kDa each) onto VP3 (approximately 60 kDa) under SPAAC conditions. To confirm that this "75 kDa" band corresponds to a nanobody-functionalized viral protein, western blot analyses were performed using an antibody specific of the nanobody structure. As depicted in Fig. 4.c, the nanobody anti-CD62L was strongly detected in the "75 kDa" band for both **rAAV2-Lys-CD62L** and **rAAV2-eTyr-CD62L**, confirming the effective formation of the nanobody-viral vector conjugate without affecting the size and structure of the nanobody. For anti-CD45, a less intense but visible recognition of the 75 kDa band was observed. Additionally, the viral origin of those same bands was further confirmed by western blot using polyclonal antibodies against VP1, VP2, and VP3 (Fig. S16.a). Importantly, all nanobody-rAAV2 conjugates reproducibly conserved the integrity of their assembled capsid and their infectivity on HeLaT cells (Fig. S16.c). Cryogenic electron microscopy (cryo-TEM), was used to evaluate the effect of nanobody conjugation on capsid geometry. As expected, a hexagonal shape was observed for unmodified rAAV2. Interestingly, outgrowths similar to "spines" were noticed (white arrows in Fig. 5.d) for the conjugated vectors **rAAV2-Lys-CD62L** and **rAAV2-eTyr-CD62L**. These specific structures were not detected in images of azido-rAAV2 (Fig. S11.c), strongly indicating the presence of covalently linked nanobodies on the capsid surface. No such outgrowths were clearly observed using the anti-CD45 nanobody, likely due to a lower level of modification (data not shown).

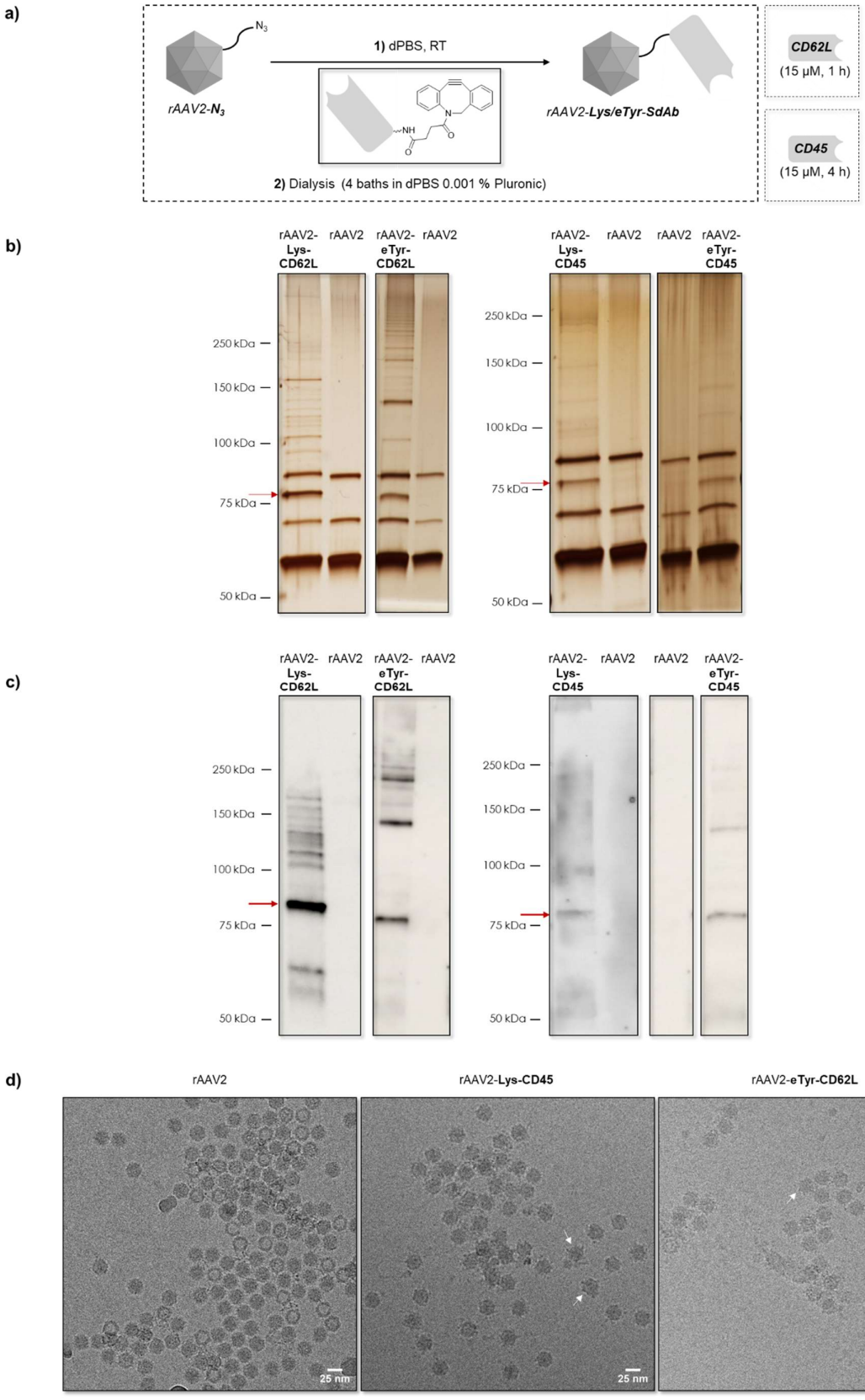

Figure 5: **SPAAC reaction on azido-rAAV2 with two DBCO-derivatized nanobodies**. a) SPAAC reaction for **rAAV2-Lys-N_3** and **rAAV2-eTyr-N_3** using two DBCO-derivatized nanobodies, one targeting CD62L and the other targeting CD45. b) Silver staining of capsid viral proteins after denaturation and SDS-PAGE migration of nanobodies modified and non-modified rAAV2 (1.5^E10 vg). c) Western blot analysis of nanobodies modified and non-modified rAAV2 to detect nanobodies structures with an anti-VHH-HRP antibody or anti-VHH-FITC antibody followed by secondary revelation using an anti-FITC-HRP antibody (1^E10 vg). d) Cryo-TEM images of rAAV2 and nanobodies modified rAAV2. Scale bars correspond to 25 nm. One representative image was chosen for each sample.

To complete biochemical characterizations, we investigated the targeting ability of the nanobody-conjugated vectors. We selected the **rAAV2-Lys-CD45** vector for transduction assays on the CD45-expressing cell line Jurkat. This cell line was chosen as this marker is highly expressed on its surface (Fig. S17). Having demonstrated that the nanobody used for rAAV labelling was efficiently interacting with this receptor (Fig. S17), Jurkat cells were infected at MOIs of 5^E2 and 1^E3. Unexpectedly, after 72 h, the number of GFP-positive cells, as observed by flow cytometry, was similar for both **rAAV2** and **rAAV2-Lys-CD45**, suggesting that the labelling did not enhance the transduction of CD45-expressing cells (Fig. 6.a). One hypothesis to explain the obtained results could be that the natural entry pathway of rAAV2 masks the one that can be induced by an interaction between CD45 and the nanobody. The rAAV of serotype 2 is using the primary receptor Heparan Sulfate ProteoGlycan (HSPG) to interact with the cells and enter into the cytoplasm[49]. Thus, to test this hypothesis, the natural entry pathway of rAAV2 was blocked by performing a heparin binding inhibition assay on Jurkat and HeLa cells (a non-expressing CD45 control cell line). In presence of 500 µg/mL of heparin, an almost full inhibition of the Jurkat cells transduction was observed with unmodified rAAV2. Indeed, the transduction efficiency observed without heparin was divided by ten (Fig. 6.b and S18). On the contrary with **rAAV2-Lys-CD45**, a residual transduction of 25 % was obtained which means that the GFP production could be partially maintained in presence of heparin**.** These encouraging observations are specific to the CD45 expressing cell line as no significant difference in the percentage of residual transduction was observed between the two vectors in HeLa cells. Furthermore, the results presented in Fig. S19 for **rAAV2-Lys-N_3** confirmed that it is not the bioconjugation reaction itself that influences this difference in transduction efficiency.

These preliminary data suggest that, in the absence of heparin, the HSPG pathway is the main entry pathway used by **rAAV2-Lys-CD45**, and that the interaction between the nanobody and the CD45 marker does not increase it. When the vector cannot interact with HSPG, the presence of the CD45 targeting moiety on the capsid partially maintains the transduction efficiency of the vector, suggesting that a new entry pathway could be used. In the light of the results, mutating arginine residues responsible for the HSPG interaction (R588 and R585) in the rAAV2 sequence [50–52] and performing the bioorthogonal sequence on those specific vectors, with more optimized SPAAC conditions, would represent a promising alternative to develop specific vectors capable of transducing only CD45 expressing cells. Ultimately, more proteins with relevant specific targeting properties would need to be conjugated to the viral capsid to study the range of cell-specific vectors and their promising

tissue-addressed tropism. We hope this will help to reduce the toxicity of gene therapy and lower the doses administrated to the patients.

To complement this study, azido conjugations and post-functionalizations were successfully conducted on rAAV8 (Fig. S20), highlighting the versatility and promising potential of chemical bioconjugation for viral capsid engineering.

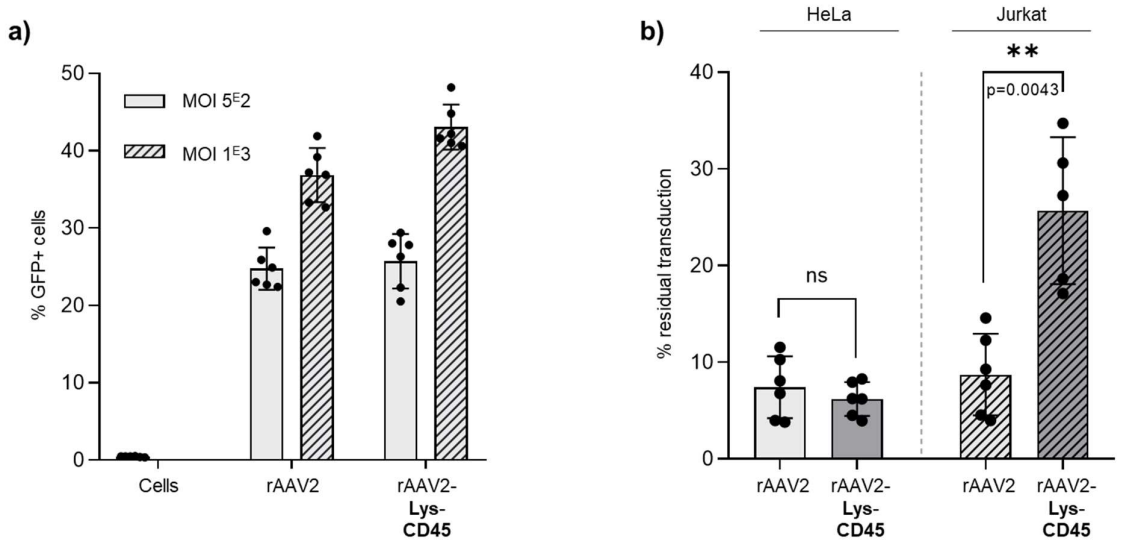

Figure 6: **Evaluation of the transduction efficiency of rAAV2-Lys-CD45 in a CD45 expressing cell line**. a) Evaluation of the transduction efficiency in Jurkat cells of rAAV2 and **rAAV2-Lys-CD45** carrying eGFP reporter gene expression cassette under the control of a ubiquitous promoter. GFP-positive Jurkat cells were quantified by flow cytometry 72 h after infection at a MOI of 5^E2 and 1^E3 (data are shown as mean ± SD of six distinct samples (n=6)). b) Evaluation of the transduction efficiency of rAAV2 and **rAAV2-Lys-CD45** in presence of 500 µg/mL of heparin in HeLaT and Jurkat cells. Both rAAV2 vectors were carrying an eGFP reporter gene expression cassette under the control of a ubiquitous promoter. GFP-positive Jurkat and HeLaT cells were quantified by flow cytometry 48 h after infection at a MOI of 5^E3 in presence of 0 µg/mL or 500 µg/mL of heparin. The results are expressed as "% residual transduction" which corresponds to the ratio between transduction in presence and in absence of heparin (data are shown as mean ± SD of six distinct samples (n=6)). Statistical significance was assessed using Mann-Whitney test (*p<0.05; **p<0.01).

CONCLUSION

We propose here a new, simple and rapid technological platform for the custom grafting of small molecules or proteins onto rAAV vectors, to improve their efficacy and specificity. To this end, we demonstrated a capsid engineering sequence initiated by chemical capsid labelling with bioorthogonal groups (azido, DBCO) and followed by an optimized SPAAC reaction. This direct and rapid sequence enabled access to rAAV-proteins conjugates from natural serotypes 2 and 8, avoiding time-consuming studies on insertion sites and production conditions (otherwise needed if proteins are genetically incorporated in the rAAV sequence). Modulated levels of functionalization can be achieved by using different bioconjugation reactions or by targeting different amino acid residues, allowing to adapt the strategy in cases of aggregation or toxicity issues with the labelling moiety. The biological interest of rAAV-protein conjugates will be further investigated in forthcoming work. Nevertheless, this study

already demonstrates that rAAV-nanobody conjugates can transduce targeted cells in presence of a rAAV binding inhibitor, which is promising for the development of highly cell-specific vectors. We expect that this bioorthogonal chemical modification of the AAV capsid will represent an easy and versatile strategy to unlock numerous challenges faced in the field of gene therapy. We also believe that this strategy may open up new applications for chemically modified capsids, using, for example, *in vivo* SPAAC reactions which have already been described in the literature with other models[53].

AKNOWLEDGMENT

The authors thank the vector core of TaRGeT, UMR 1089 (CPV, INSERM and Nantes Université, which is a bioproduction and biotherapy national integrator (ANR-22-AIBB-0001), http://umr1089.univ-nantes.fr) for the production of the rAAV vectors used in this study. This research was supported by the Fondation d'Entreprise Thérapie Génique en Pays de Loire, the Centre Hospitalier Universitaire (CHU) of Nantes, the Institut National de la Santé et de la Recherche Médicale (INSERM), Nantes Université, and by grants from the French National Agency for Research ChemAAV (ANR-19-CE18-0001)). The authors acknowledge the Cytocell core facility (SFR Bonamy, UMS BioCore, Nantes, France) for its technical expertise and assistance. Cytocell is a member of the *Groupement d'Intérêt Scientifique* Biogenouest and is part of the Labex IGO program that is supported by the *Agence Nationale de la Recherche* (n°ANR-11-LABX-0016-01).

Credit authorship contribution statement

Maia Marchand (Conceptualization; Methodology; Writing – original draft; Writing – review & editing), Mohammed Bouzelha (Conceptualization; Methodology; Validation), Sébastien Depienne (Conceptualization; Methodology; Visualization; Writing – original draft), Karine Pavageau (Methodology; Validation), Roxanne Peumery (Methodology), Denis Loquet (Methodology), Dimitri Alvarez-Dorta (Methodology; Validation), Mickaël Guilbaud (Methodology; Validation), Mikaël Croyal (Methodology; Validation), Aurélien Dupont (Methodology; Validation), Oumeya Adjali (Funding acquisition; Project administration; Resources; Supervision), Sébastien G. Gouin (Supervision; Writing – original draft), David Deniaud (Conceptualization; Funding acquisition; Methodology; Resources; Validation; Writing – original draft; Writing – review & editing), Mathieu Mével (Funding acquisition; Supervision; Validation; Writing – original draft; Writing – review & editing).

Conflicts of interest

M.M., D.D., S.G.G. and S.D. are inventors on patents including the technology described in this manuscript. No potential conflicts of interest were disclosed.

Data availability

All relevant data are available from the authors on request and are included within the manuscript.

Appendix A. Supplementary data

Experimental procedures, chemical synthesis, ^{1}H NMR, ^{13}C NMR, supplementary figures and gating strategies.

REFERENCES

(1) Kuzmin, D. A.; Shutova, M. V.; Johnston, N. R.; Smith, O. P.; Fedorin, V. V.; Kukushkin, Y. S.; van der Loo, J. C. M.; Johnstone, E. C. The Clinical Landscape for AAV Gene Therapies. *Nature Reviews Drug Discovery* **2021**, *20* (3), 173–174. https://doi.org/10.1038/d41573-021-00017-7.

(2) Kang, L.; Jin, S.; Wang, J.; Lv, Z.; Xin, C.; Tan, C.; Zhao, M.; Wang, L.; Liu, J. AAV Vectors Applied to the Treatment of CNS Disorders: Clinical Status and Challenges. *Journal of Controlled Release* **2023**, *355*, 458–473. https://doi.org/10.1016/j.jconrel.2023.01.067.

(3) Pupo, A.; Fernández, A.; Low, S. H.; François, A.; Suárez-Amarán, L.; Samulski, R. J. AAV Vectors: The Rubik's Cube of Human Gene Therapy. *Molecular Therapy* **2022**. https://doi.org/10.1016/j.ymthe.2022.09.015.

(4) Zabaleta, N.; Unzu, C.; Weber, N. D.; Gonzalez-Aseguinolaza, G. Gene Therapy for Liver Diseases — Progress and Challenges. *Nat Rev Gastroenterol Hepatol* **2023**, *20* (5), 288–305. https://doi.org/10.1038/s41575-022-00729-0.

(5) Drag, S.; Dotiwala, F.; Upadhyay, A. K. Gene Therapy for Retinal Degenerative Diseases: Progress, Challenges, and Future Directions. *Investigative Ophthalmology & Visual Science* **2023**, *64* (7), 39. https://doi.org/10.1167/iovs.64.7.39.

(6) Brooks, P. J.; Urv, T. K.; Parisi, M. A. Gene-Targeted Therapies: Overview and Implications. *American Journal of Medical Genetics Part C: Seminars in Medical Genetics* **2023**, *193* (1), 13–18. https://doi.org/10.1002/ajmg.c.32033.

(7) Wu, Z.; Asokan, A.; Samulski, R. J. Adeno-Associated Virus Serotypes: Vector Toolkit for Human Gene Therapy. *Molecular Therapy* **2006**, *14* (3), 316–327. https://doi.org/10.1016/j.ymthe.2006.05.009.

(8) Issa, S. S.; Shaimardanova, A. A.; Solovyeva, V. V.; Rizvanov, A. A. Various AAV Serotypes and Their Applications in Gene Therapy: An Overview. *Cells* **2023**, *12* (5), 785. https://doi.org/10.3390/cells12050785.

(9) Gray, S. J.; Matagne, V.; Bachaboina, L.; Yadav, S.; Ojeda, S. R.; Samulski, R. J. Preclinical Differences of Intravascular AAV9 Delivery to Neurons and Glia: A Comparative Study of Adult Mice and Nonhuman Primates. *Molecular Therapy* **2011**, *19* (6), 1058–1069. https://doi.org/10.1038/mt.2011.72.

(10) Ertl, H. C. J. Immunogenicity and Toxicity of AAV Gene Therapy. *Frontiers in Immunology* **2022**, *13*.

(11) Young, P. Treatment to Cure: Advancing AAV Gene Therapy Manufacture. *Drug Discovery Today* **2023**, *28* (7), 103610. https://doi.org/10.1016/j.drudis.2023.103610.

(12) Kimura, K.; Nagai, Y.; Hatanaka, G.; Fang, Y.; Tanabe, S.; Zheng, A.; Fujiwara, M.; Nakano, M.; Hori, Y.; Takeuchi, R. F.; Inagaki, M.; Minamimoto, T.; Fujita, I.; Inoue, K.-I.; Takada, M. A Mosaic Adeno-Associated Virus Vector as a Versatile Tool That Exhibits

High Levels of Transgene Expression and Neuron Specificity in Primate Brain. *Nat Commun* **2023**, *14* (1), 4762. https://doi.org/10.1038/s41467-023-40436-1.
(13) Viney, L.; Bürckstümmer, T.; Eddington, C.; Mietzsch, M.; Choudhry, M.; Henley, T.; Agbandje-McKenna, M. Adeno-Associated Virus (AAV) Capsid Chimeras with Enhanced Infectivity Reveal a Core Element in the AAV Genome Critical for Both Cell Transduction and Capsid Assembly. *Journal of Virology* **2021**, *95* (7), 10.1128/jvi.02023-20. https://doi.org/10.1128/jvi.02023-20.
(14) Goertsen, D.; Goeden, N.; Flytzanis, N. C.; Gradinaru, V. Targeting the Lung Epithelium after Intravenous Delivery by Directed Evolution of Underexplored Sites on the AAV Capsid. *Mol Ther Methods Clin Dev* **2022**, *26*, 331–342. https://doi.org/10.1016/j.omtm.2022.07.010.
(15) Grimm, D.; Lee, J. S.; Wang, L.; Desai, T.; Akache, B.; Storm, T. A.; Kay, M. A. In Vitro and In Vivo Gene Therapy Vector Evolution via Multispecies Interbreeding and Retargeting of Adeno-Associated Viruses. *Journal of Virology* **2008**, *82* (12), 5887–5911. https://doi.org/10.1128/JVI.00254-08.
(16) Chan, K. Y.; Jang, M. J.; Yoo, B. B.; Greenbaum, A.; Ravi, N.; Wu, W.-L.; Sánchez-Guardado, L.; Lois, C.; Mazmanian, S. K.; Deverman, B. E.; Gradinaru, V. Engineered AAVs for Efficient Noninvasive Gene Delivery to the Central and Peripheral Nervous Systems. *Nat Neurosci* **2017**, *20* (8), 1172–1179. https://doi.org/10.1038/nn.4593.
(17) Liguore, W. A.; Domire, J. S.; Button, D.; Wang, Y.; Dufour, B. D.; Srinivasan, S.; McBride, J. L. AAV-PHP.B Administration Results in a Differential Pattern of CNS Biodistribution in Non-Human Primates Compared with Mice. *Molecular Therapy* **2019**, *27* (11), 2018–2037. https://doi.org/10.1016/j.ymthe.2019.07.017.
(18) Chang, H.; Du, A.; Jiang, J.; Ren, L.; Liu, N.; Zhou, X.; Liang, J.; Gao, G.; Wang, D. Non-Canonical Amino Acid Incorporation into AAV5 Capsid Enhances Lung Transduction in Mice. *Molecular Therapy - Methods & Clinical Development* **2023**, 101129. https://doi.org/10.1016/j.omtm.2023.101129.
(19) Ried, M. U.; Girod, A.; Leike, K.; Büning, H.; Hallek, M. Adeno-Associated Virus Capsids Displaying Immunoglobulin-Binding Domains Permit Antibody-Mediated Vector Retargeting to Specific Cell Surface Receptors. *Journal of Virology* **2002**, *76* (9), 4559–4566. https://doi.org/10.1128/jvi.76.9.4559-4566.2002.
(20) Sayroo, R.; Nolasco, D.; Yin, Z.; Colon-Cortes, Y.; Pandya, M.; Ling, C.; Aslanidi, G. Development of Novel AAV Serotype 6 Based Vectors with Selective Tropism for Human Cancer Cells. *Gene Ther* **2016**, *23* (1), 18–25. https://doi.org/10.1038/gt.2015.89.
(21) Katrekar, D.; Moreno, A. M.; Chen, G.; Worlikar, A.; Mali, P. Oligonucleotide Conjugated Multi-Functional Adeno-Associated Viruses. *Sci Rep* **2018**, *8* (1), 3589. https://doi.org/10.1038/s41598-018-21742-x.
(22) Kelemen, R. E.; Mukherjee, R.; Cao, X.; Erickson, S. B.; Zheng, Y.; Chatterjee, A. A Precise Chemical Strategy To Alter the Receptor Specificity of the Adeno-Associated Virus. *Angewandte Chemie International Edition* **2016**, *55* (36), 10645–10649. https://doi.org/10.1002/anie.201604067.
(23) Erickson, S. B.; Pham, Q.; Cao, X.; Glicksman, J.; Kelemen, R. E.; Shahraeini, S. S.; Bodkin, S.; Kiyam, Z.; Chatterjee, A. Precise Manipulation of the Site and Stoichiometry of Capsid Modification Enables Optimization of Functional Adeno-Associated Virus Conjugates. *Bioconjugate Chem.* **2023**. https://doi.org/10.1021/acs.bioconjchem.3c00411.
(24) Puzzo, F.; Zhang, C.; Gray, B. P.; Zhang, F.; Sullenger, B. A.; Kay, M. A. Aptamer-Programmable Adeno-Associated Viral Vectors as a Novel Platform for Cell-Specific Gene Transfer. *Molecular Therapy - Nucleic Acids* **2023**, S2162253123000100. https://doi.org/10.1016/j.omtn.2023.01.007.
(25) Pham, Q.; Glicksman, J.; Chatterjee, A. Chemical Approaches to Probe and Engineer AAV Vectors. *Nanoscale* **2024**. https://doi.org/10.1039/D4NR01300J.
(26) Münch, R. C.; Janicki, H.; Völker, I.; Rasbach, A.; Hallek, M.; Büning, H.; Buchholz, C. J. Displaying High-Affinity Ligands on Adeno-Associated Viral Vectors Enables Tumor Cell-Specific and Safe Gene Transfer. *Molecular Therapy* **2013**, *21* (1), 109–118. https://doi.org/10.1038/mt.2012.186.

(27) Wu, P.; Xiao, W.; Conlon, T.; Hughes, J.; Agbandje-McKenna, M.; Ferkol, T.; Flotte, T.; Muzyczka, N. Mutational Analysis of the Adeno-Associated Virus Type 2 (AAV2) Capsid Gene and Construction of AAV2 Vectors with Altered Tropism. *Journal of Virology* **2000**, *74* (18), 8635–8647. https://doi.org/10.1128/jvi.74.18.8635-8647.2000.
(28) Mével, M.; Bouzelha, M.; Leray, A.; Pacouret, S.; Guilbaud, M.; Penaud-Budloo, M.; Alvarez-Dorta, D.; Dubreil, L.; G. Gouin, S.; Philippe Combal, J.; Hommel, M.; Gonzalez-Aseguinolaza, G.; Blouin, V.; Moullier, P.; Adjali, O.; Deniaud, D.; Ayuso, E. Chemical Modification of the Adeno-Associated Virus Capsid to Improve Gene Delivery. *Chemical Science* **2020**, *11* (4), 1122–1131. https://doi.org/10.1039/C9SC04189C.
(29) Seo, J. W.; Ingham, E. S.; Mahakian, L.; Tumbale, S.; Wu, B.; Aghevlian, S.; Shams, S.; Baikoghli, M.; Jain, P.; Ding, X.; Goeden, N.; Dobreva, T.; Flytzanis, N. C.; Chavez, M.; Singhal, K.; Leib, R.; James, M. L.; Segal, D. J.; Cheng, R. H.; Silva, E. A.; Gradinaru, V.; Ferrara, K. W. Positron Emission Tomography Imaging of Novel AAV Capsids Maps Rapid Brain Accumulation. *Nat Commun* **2020**, *11* (1), 2102. https://doi.org/10.1038/s41467-020-15818-4.
(30) Leray, A.; Lalys, P.-A.; Varin, J.; Bouzelha, M.; Bourdon, A.; Alvarez-Dorta, D.; Pavageau, K.; Depienne, S.; Marchand, M.; Mellet, A.; Demilly, J.; Ducloyer, J.-B.; Girard, T.; Fraysse, B.; Ledevin, M.; Guilbaud, M.; Gouin, S. G.; Ayuso, E.; Adjali, O.; Larcher, T.; Cronin, T.; Le Guiner, C.; Deniaud, D.; Mével, M. Novel Chemical Tyrosine Functionalization of Adeno-Associated Virus Improves Gene Transfer Efficiency in Liver and Retina. *Biomedicine & Pharmacotherapy* **2024**, *171*, 116148. https://doi.org/10.1016/j.biopha.2024.116148.
(31) Depienne, S.; Bouzelha, M.; Courtois, E.; Pavageau, K.; Lalys, P.-A.; Marchand, M.; Alvarez-Dorta, D.; Nedellec, S.; Marín-Fernández, L.; Grandjean, C.; Boujtita, M.; Deniaud, D.; Mével, M.; Gouin, S. G. Click-Electrochemistry for the Rapid Labeling of Virus, Bacteria and Cell Surfaces. *Nat Commun* **2023**, *14* (1), 1–10. https://doi.org/10.1038/s41467-023-40534-0.
(32) Devaraj, N. K. The Future of Bioorthogonal Chemistry. *ACS Cent. Sci.* **2018**, *4* (8), 952–959. https://doi.org/10.1021/acscentsci.8b00251.
(33) Penninger, J. M.; Irie-Sasaki, J.; Sasaki, T.; Oliveira-dos-Santos, A. J. CD45: New Jobs for an Old Acquaintance. *Nat Immunol* **2001**, *2* (5), 389–396. https://doi.org/10.1038/87687.
(34) Rainer, T. H. L-Selectin in Health and Disease. *Resuscitation* **2002**, *52* (2), 127–141. https://doi.org/10.1016/S0300-9572(01)00444-0.
(35) Mével, M.; Pichard, V.; Bouzelha, M.; Alvarez-Dorta, D.; Lalys, P.-A.; Provost, N.; Allais, M.; Mendes, A.; Landagaray, E.; Ducloyer, J.-B.; Toublanc, E.; Galy, A.; Brument, N.; Lefevre, G. M.; Gouin, S. G.; Isiegas, C.; Meur, G. L.; Cronin, T.; Guiner, C. L.; Weber, M.; Moullier, P.; Ayuso, E.; Deniaud, D.; Adjali, O. Mannose-Coupled AAV2: A Second-Generation AAV Vector for Increased Retinal Gene Therapy Efficiency. *Molecular Therapy. Methods & Clinical Development* **2024**, *32* (1). https://doi.org/10.1016/j.omtm.2024.101187.
(36) Budin, G.; Dimala, M. M.; Lamour, V.; Oudet, P.; Mioskowski, C.; Meunier, S.; Brino, L.; Wagner, A. A Chemical Labeling Strategy for Proteomics under Nondenaturing Conditions. *ChemBioChem* **2010**, *11* (1), 79–82. https://doi.org/10.1002/cbic.200900641.
(37) Goswami, L. N.; Houston, Z. H.; Sarma, S. J.; Jalisatgi, S. S.; Hawthorne, M. F. Efficient Synthesis of Diverse Heterobifunctionalized Clickable Oligo(Ethylene Glycol) Linkers: Potential Applications in Bioconjugation and Targeted Drug Delivery. *Org. Biomol. Chem.* **2013**, *11* (7), 1116–1126. https://doi.org/10.1039/C2OB26968F.
(38) Depienne, S.; Alvarez-Dorta, D.; Croyal, M.; T. Temgoua, R. C.; Charlier, C.; Deniaud, D.; Mével, M.; Boujtita, M.; G. Gouin, S. Luminol Anchors Improve the Electrochemical-Tyrosine-Click Labelling of Proteins. *Chemical Science* **2021**, *12* (46), 15374–15381. https://doi.org/10.1039/D1SC04809K.
(39) Rose, J. A.; Maizel, J. V.; Inman, J. K.; Shatkin, A. J. Structural Proteins of Adenovirus-Associated Viruses. *Journal of Virology* **1971**, *8* (5), 766–770. https://doi.org/10.1128/jvi.8.5.766-770.1971.

(40) Dommerholt, J.; Rutjes, F. P. J. T.; van Delft, F. L. Strain-Promoted 1,3-Dipolar Cycloaddition of Cycloalkynes and Organic Azides. *Top Curr Chem (Z)* **2016**, *374* (2), 16. https://doi.org/10.1007/s41061-016-0016-4.
(41) Dundas, C. M.; Demonte, D.; Park, S. Streptavidin–Biotin Technology: Improvements and Innovations in Chemical and Biological Applications. *Appl Microbiol Biotechnol* **2013**, *97* (21), 9343–9353. https://doi.org/10.1007/s00253-013-5232-z.
(42) D'Souza, A. A.; Devarajan, P. V. Asialoglycoprotein Receptor Mediated Hepatocyte Targeting - Strategies and Applications. *J Control Release* **2015**, *203*, 126–139. https://doi.org/10.1016/j.jconrel.2015.02.022.
(43) Lang, K.; Chin, J. W. Cellular Incorporation of Unnatural Amino Acids and Bioorthogonal Labeling of Proteins. *Chem. Rev.* **2014**, *114* (9), 4764–4806. https://doi.org/10.1021/cr400355w.
(44) Kontermann, R. E.; Brinkmann, U. Bispecific Antibodies. *Drug Discovery Today* **2015**, *20* (7), 838–847. https://doi.org/10.1016/j.drudis.2015.02.008.
(45) Jain, M.; Kamal, N.; Batra, S. K. Engineering Antibodies for Clinical Applications. *Trends in Biotechnology* **2007**, *25* (7), 307–316. https://doi.org/10.1016/j.tibtech.2007.05.001.
(46) Jovčevska, I.; Muyldermans, S. The Therapeutic Potential of Nanobodies. *BioDrugs* **2020**, *34* (1), 11–26. https://doi.org/10.1007/s40259-019-00392-z.
(47) Ivetic, A.; Hoskins Green, H. L.; Hart, S. J. L-Selectin: A Major Regulator of Leukocyte Adhesion, Migration and Signaling. *Front. Immunol.* **2019**, *10*. https://doi.org/10.3389/fimmu.2019.01068.
(48) Saunders, A. E.; Johnson, P. Modulation of Immune Cell Signalling by the Leukocyte Common Tyrosine Phosphatase, CD45. *Cellular Signalling* **2010**, *22* (3), 339–348. https://doi.org/10.1016/j.cellsig.2009.10.003.
(49) Summerford, C.; Samulski, R. J. Membrane-Associated Heparan Sulfate Proteoglycan Is a Receptor for Adeno-Associated Virus Type 2 Virions. *Journal of Virology* **1998**, *72* (2), 1438–1445. https://doi.org/10.1128/jvi.72.2.1438-1445.1998.
(50) Kern, A.; Schmidt, K.; Leder, C.; Müller, O. J.; Wobus, C. E.; Bettinger, K.; Von der Lieth, C. W.; King, J. A.; Kleinschmidt, J. A. Identification of a Heparin-Binding Motif on Adeno-Associated Virus Type 2 Capsids. *Journal of Virology* **2003**, *77* (20), 11072–11081. https://doi.org/10.1128/jvi.77.20.11072-11081.2003.
(51) Erickson, S. B.; Mukherjee, R.; Kelemen, R. E.; Wrobel, C. J. J.; Cao, X.; Chatterjee, A. Precise Photoremovable Perturbation of a Virus–Host Interaction. *Angewandte Chemie International Edition* **2017**, *56* (15), 4234–4237. https://doi.org/10.1002/anie.201700683.
(52) Opie, S. R.; Warrington, K. H.; Agbandje-McKenna, M.; Zolotukhin, S.; Muzyczka, N. Identification of Amino Acid Residues in the Capsid Proteins of Adeno-Associated Virus Type 2 That Contribute to Heparan Sulfate Proteoglycan Binding. *Journal of Virology* **2003**, *77* (12), 6995–7006. https://doi.org/10.1128/JVI.77.12.6995-7006.2003.
(53) Wang, H.; Sobral, M. C.; Zhang, D. K. Y.; Cartwright, A. N.; Li, A. W.; Dellacherie, M. O.; Tringides, C. M.; Koshy, S. T.; Wucherpfennig, K. W.; Mooney, D. J. Metabolic Labeling and Targeted Modulation of Dendritic Cells. *Nat. Mater.* **2020**, *19* (11), 1244–1252. https://doi.org/10.1038/s41563-020-0680-1.

TABLE OF CONTENTS GRAPHIC